Volume 12

Washington University
Undergraduate Research Digest

Spring 2017

Strong Coupling of a Spin Ensemble in Ruby Crystal to a Three-Dimensional Copper Cavity

Michael Seitanakis
Washington University in St. Louis

Strong Coupling of a Spin Ensemble in Ruby Crystal to a Three-Dimensional Copper Cavity

Author:

Michael Seitanakis

Michael majored in Physics, graduating with College Honors from the College of Arts & Sciences at Washington University in St. Louis in May 2017. Next year he will work for Epic Systems Corporation in medical software with the eventual plan of pursuing a graduate degree in physics.

KEY TERMS

- Electron-spin ensemble
- Three-dimensional double post reentrant copper cavity
- Qubit
- Quantum computer

ABSTRACT

In the pursuit of developing quantum technology, researchers study novel ways to measure and control quantum phenomena. For example, if strong enough coupling is attained with the spin ensemble in a ruby crystal that has a small enough linewidth, this system could serve in a quantum computer as a quantum memory. Previous research has shown strong coupling to spin ensembles, but achieving a smaller spin linewidth is required to create quantum memory devices. This study examines the coupling between a spin ensemble and a double post reentrant three-dimensional copper cavity, which could take advantage of its higher mode volume and a more constant magnetic field through the ruby volume to achieve higher coupling and a smaller spin linewidth. Measuring the transmittance through the cavity, the change in quality factor, Q, and resonant frequency of the cavity indicate coupling strength, g, and the spin linewidth. As the advent of the quantum computer nears, this research adds to the body of work that attempts to access the vast expanse of Hilbert space.

FACULTY MENTOR: KATER MURCH, PH.D.
ASSISTANT PROFESSOR OF PHYSICS

Dr. Kater Murch's research group conducts experimental research at the interface of atomic, molecular, optical, and condensed matter physics. They use nano-fabrication techniques to construct superconducting quantum circuits that allow them to probe fundamental questions in quantum mechanics.

ACKNOWLEDGEMENTS

I thank my research mentor Dr. Kater Murch for his guidance on this project and in my development as a scientist. I would also like to thank Patrick Harrington, Mehti Naghiloo, and Dian Tan for their insightful discussions. Finally, I thank my cohort in the lab, the Under(grad) Achievers for such a fun summer.

Peer Editors:

Chase Antonacci, a sophomore majoring in Philosophy-Neuroscience-Psychology

Kelsey Pitts, a senior majoring in Biochemistry

INTRODUCTION

The successful development of a quantum computer would be "more revolutionary than anything before, including the classical computer and the internet"[1]. Research in quantum computing consists of creating and developing technology that measure and control quantum phenomena in diverse physical systems. Each device has its advantages and disadvantages, suggesting the need for a quantum computer made of different integrated components with different specializations. For example, much research has been conducted on the precise measurement, fast control, and efficient coupling of the transmon qubit[2]; however researchers cannot overcome the shortcoming that quantum information disappears quickly when stored in a transmon relative to computation time. To circumvent the issue of information loss in transmons, recent research has gone into developing quantum memory devices, which store quantum information for long amounts of time (relative to the computation time). Spin ensembles in ruby hold information much longer than fast-processing transmon qubits[4] and they also have a resonance in the energy range of transmons, which suggests direct coupling is feasible. Current research attempts to develop different devices that access the ruby spin ensemble through electromagnetic coupling[6]. Previous works have achieved strong coupling, but the spin linewidth was too wide for the quantum information storage application[6]. We hypothesized that a three-dimensional double post reentrant cavity would achieve strong coupling to the ruby spin ensemble since it can focus the magnetic field within the ruby, and would have better spin linewidth. To test the coupling, we designed a cavity and ruby shape to maximize magnetic coupling, measuring the change in cavity resonance and quality factor as an external magnetic field changed the ruby spin ensemble resonance. Achieving strong coupling between the cavity and this spin ensemble along with finding a larger spin ensemble quality factor would lead to further research in coupling ruby spins to other quantum systems like transmon qubits. A benefit of the 3D cavity is the potential to couple the ruby spins with part of the cavity mode to transmon qubits with another part of the cavity mode. The strong coupling found in this experiment shows promise in this cavity's ability to control ruby spins and eventually couple them to transmon qubits or other components like them.

II COUPLED OSCILLATORS

This summer I studied coupled oscillators, systems that store energy in each of their oscillators as well as in the interactions between the two. This interaction, or coupling, allows experimentalists to follow a simple line of logic that leads to amazing discoveries: if I can measure oscillator *A* and oscillator *A* is coupled to oscillator *B*, then I can indirectly learn information about oscillator *B*. Later Section III describes the physics of the two oscillators that I studied, a spin ensemble in ruby and a resonant cavity. However, first I will start by describing coupled harmonic oscillators, a simplified case. A more detailed description of coupled oscillators can be found in most classical dynamics texts[5].

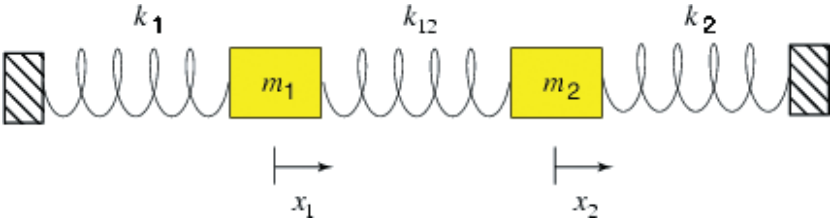

Figure 1: Schematic of Two Masses Attached to Simple Springs Oscillating without Friction.

Spring with constant k_1 (k_2) attaches mass m_1 (m_2) to a fixed wall on the left (right). A third spring of constant k_{12} couples the two masses in the middle. Define the position of m_1 and m_2 as x_1 and x_2 respectively where $x_1 = x_2 = 0$ at equilibrium.

Consider a system of two masses, m_1 and m_2, connected to fixed walls with simple springs of Hooke's constant k_1 and k_2 respectively and connected to each other with a simple spring of constant k_{12} as shown in *Figure 1*. In order to explore the motion of the masses in this system, one can write down Newton's law for m_1 and m_2:

$$\begin{aligned} m_1\ddot{x}_1 &= -(k_1 + k_{12})x_1 + k_{12}x_2 \\ m_2\ddot{x}_2 &= -(k_2 + k_{12})x_2 + k_{12}x_1 \end{aligned} \tag{1}$$

To solve the equations of motion, one can use the ansatz

$$\begin{aligned} x_1 &= B_1 e^{i\omega t} \\ x_2 &= B_2 e^{i\omega t} \end{aligned} \tag{2}$$

where ω describes a radial frequency at which both masses could sinusoidally oscillate in the steady state, ignoring friction, and B_1 and B_2 are complex numbers that contain the amplitude and phase of each mass' oscillation. Plugging in the guessed forms of x_1 and x_2, the equations of motion become

$$\begin{aligned} B_1(k_1 + k_{12} - m_1\omega^2) - B_2k_{12} &= 0 \\ -B_1k_{12} + B_2(k_2 + k_{12} - m_2\omega^2) &= 0 \end{aligned} \tag{3}$$

Observing that these coupled linear equations can be written in matrix form, the possible values for ω that would satisfy both equations would also cause the determinant of the coefficients of B_1 and B_2 to vanish:

$$det \begin{vmatrix} (k_1 + k_{12} - m_1\omega^2) & -k_{12} \\ -k_{12} & (k_2 + k_{12} - m_2\omega^2) \end{vmatrix} = 0 \tag{4}$$

Since the determinant yields a quadratic equation in ω^2, this system has two possible steady state frequencies.

This mathematical framework predicts the results of experiments. For example, let's say we want to know the effect of changing k_1 (i.e., making the first spring tighter) on the possible steady state frequencies of the system, $\omega(k_1)$ while holding all other parameters constant. After some careful algebra, one can isolate ω^2 and put it in terms of k_1. The resulting equation takes the form of a hyperbola with one asymptote parallel to the *x*-axis:

$$y = a(x - c) + d \pm \sqrt{a^2(x - c)^2 + g^2} \tag{5}$$

where each constant has graphical meaning as shown in *Figure 2*.

To understand *Figure 2*, first notice that the limit where *y* becomes its asymptotes, $g \rightarrow 0$, represents the situation of two decoupled oscillators. In this limit, the line of zero slope would represent the frequency of oscillating mass m_2, unaffected by the changing spring constant k_1, and the sloped line would represent the frequency of mass m_1, linearly dependent on k_1. As coupling increases, the spacing between the frequencies increases at the crossing. This avoided crossing spacing, *g*, allows for a good measurement of coupling strength between two oscillators; larger spacing implies stronger coupling.

Thinking about the physics of the system as you sweep through k_1 values leads to interesting places. When k_1 is far from the crossing region, the values for ω closely match the asymptotes, the frequencies when the oscillators are decoupled. In this range of k_1, one can think of the oscillators as roughly separate, they do not have a great affect on each other, as seen by the small change in ω. However when k_1 is in the crossing region, the coupled resonances differ much more from the decoupled resonances. For this range of k_1, one can no longer think of the oscillators as separate. They now behave as a hybrid oscillator that has distinct modes compared to its separate parts.

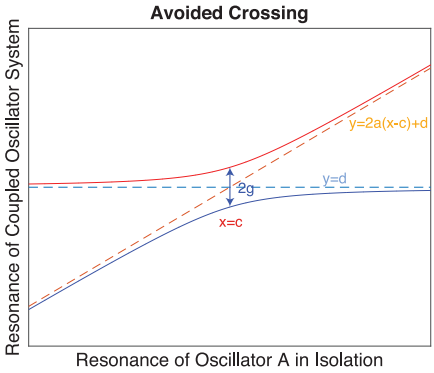

Figure 2: Avoided Crossing Graph of Equation 5

The asymptotes of the hyperbola $y = d$ and $y = 2a(x - c)+d$ represent the modes of the two oscillators if the spring with constant k_{12}did not exist. The gap between *y* values where the two asymptotes cross indicates coupling strength. Notice the *y* values nearly match the asymptotes far away from the intersection, but greatly differ near the intersection. Physically this relationship means that the oscillators act like decoupled oscillators far from where their modes cross, and the coupling shows most strongly near the cross.

The following sections focus on an experiment that uses the coupled oscillator model. You might find it useful to refer back to this section and draw analogies to the mass and spring model.

III COUPLING SPIN MODES IN A RUBY CRYSTAL TO A COPPER CAVITY

This section describes an actual experiment that follows the theoretical framework laid out in Section II. An ensemble of spins in a ruby crystal plays the role of one oscillator, the other, a three dimensional copper cavity resonator. The electromagnetic field mediates an interaction between the spin ensemble and cavity. First I will describe the physics of the two oscillators separately, then I will describe their coupling and the experiment that follows.

A. Spin Ensemble In Ruby

Ruby is composed of a lattice of Al_2O_3 with chromium ions infrequently replacing the Aluminum in the lattice (*Figure 3*). Chromium electrons exist in orbital states with angular momentum and a dipole moment that follow the dynamics of a spin-$\frac{3}{2}$ quantum system. Since the chromium ions are spin-$\frac{3}{2}$ fermions, there are two dominant interactions between Cr^{+3} ions: magnetic dipole-dipole coupling and the exchange interaction. The derivation by Stancil in *Quantum Theory of Spin Waves*[7] predicts that the wavelength of the resonance determines which of these two interactions dominates: wavelengths much longer than spin spacing follow dipole dynamics and wavelengths on the order of spin spacing follow the exclusion interaction. The wavelength of our ruby's resonance suggests that the exclusion interaction dominates.

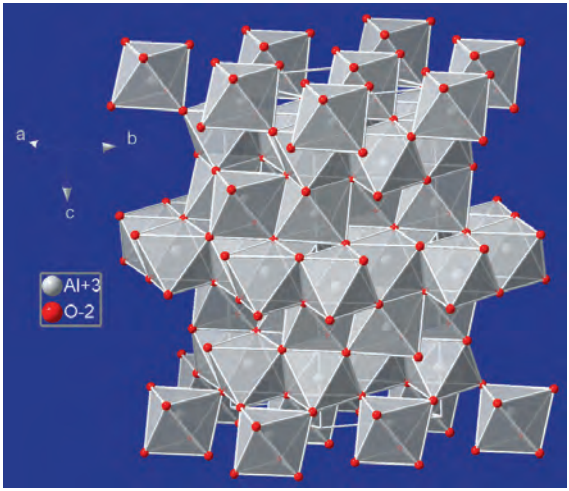

Figure. 3: Ideal Lattice of a Ruby Crystal
Some Al^{+3} sites are replaced by Cr^{+3}, differentiating the ruby crystal from sapphire, which consists of pure Al_2O_3.

In a thorough description of the exclusion interaction and spin dynamics, Stancil's *Quantum Theory of Spin Waves*[7] derives many fundamental spin dynamics from the hydrogen atom to a three dimensional magnon system. To model a lattice of exclusion-interaction-coupled spins, Stancil combines the Heisenberg Hamiltonian with the Zeeman Hamiltonian:

$$\mathcal{H} = -2\frac{\mathcal{J}}{\hbar^2}\sum_{j,\boldsymbol{\delta}} \mathbf{S}_j \cdot \mathbf{S}_{j+\boldsymbol{\delta}} - \frac{g\mu_B B_0}{\hbar}\sum_j S_{jz} \tag{6}$$

The Heisenberg Hamiltonian encapsulates the exclusion energies between each pair of nearest-neighbor spins (the first term), and the Zeeman Hamiltonian represents the energy of dipole orientations in an external field B_0 (the second term). The index j represents a specific spin site in the crystal, and the vector $\boldsymbol{\delta}$ represents a vector to one of the nearest neighbors of spin j. The Heisenberg Hamiltonian comes from the exclusion interaction between spins which depends on only the relative orientation of the spins, as shown by the prefactor

$$\mathcal{J} = \tfrac{1}{2}(\varepsilon_S - \varepsilon_T) \tag{7}$$

where $\varepsilon_{S(T)}$ is the energy of the symmetric (antisymmetric) spin orientation. The Zeeman Hamiltonian, on the other hand, depends on the strength of the external magnetic field, B_0. Stancil goes on to derive a mathmatical analogy of this 3D system to a harmonic oscillator with quantized energy levels. Solving the eigen problem for this Hamiltonian leads to discrete energy levels of the oscillator for a given wavevector $\boldsymbol{\kappa}$:

$$\hbar\omega_\kappa = 4\mathcal{J}sZ(1-\gamma_\kappa) + g\mu_B B_0 \tag{8}$$

where s is an integer and Z and γ_κ depend on the relative orientation of the spins. Most importantly for this experiment, the Zeeman term causes *the energy levels to depend linearly on external magnetic field* B_0. This means that the resonant frequency of the spin ensemble (a harmonic oscillator) can be changed by a changing magnetic field enabling us to conduct the experiment described in Section II.

B. Resonant Copper Cavity

Although the spin ensemble described in Section III A exhibits amazing solid state physics, measuring the resonator requires clever experimental design. Because spin is a magnetic phenomenon, external electromagnetic excitations would affect the spin ensemble. A resonant conducting cavity provides a well understood, measurable oscillating field that can affect the spin dynamics and therefore couple to the ruby resonator.

Before diving into how a cavity interacts with the ruby spin ensemble, first let's consider a cavity in isolation. Solving Maxwell's equations for a given geometry of a conducting cavity allows one to explore the resonance and shape of its electromagnetic modes. Griffiths[3] describes the boundary conditions and solutions to such problems in much more detail. Briefly, since the exterior of the cavity is assumed to be perfectly conducting, $\mathbf{E} = \mathbf{0}$ around the boundaries. The following boundary condition applies just inside the walls of the cavity:

$$\mathbf{E}^{\parallel} = \mathbf{0} \tag{9}$$

Assuming sinusoidally time varying solutions of **E** and **B**, one can solve the relevant Maxwell's equations by applying the boundary conditions. To solve complicated cavities, one can use software like HFSS to approximate the time-varying fields for different modes. Notice a few features of the simulations shown in *Figures 4*, *5* and *6* that guide the design of a useful cavity shape: 1) E-field is perpendicular to B-field at any point 2) E-field maxima and B-field maxima occur at different coordinates. 3) One can identify patterns like the E-field of a parallel plate capacitor where there are two close flat metal surfaces and the B-field of a current carrying wire around the side of an extrusion.

In order to strongly couple the magnetic field of the cavity to the magnetic spins of the ruby, the maximum magnetic field in the cavity should occur inside the volume of the ruby. In fact, ideally all of the magnetic mode volume occurs in the ruby while all of the electric mode volume avoids it. The electric field should avoid the volume of the ruby because the crystal is a dielectric which causes damping in oscillations of the electric field. Our experiment used the double post cavity in *Figure 6*. Most of the magnetic field occurs between the two posts, where the rectangular shaped ruby is inserted. The electric field mostly occurs outside of the ruby, minimizing loss. The HFSS simulation also suggests where to put the probes that couple the cavity to our measurement ports. These probes couple to the electric field of the cavity, so they are placed where the electric field resides: between the roof and the top of the posts.

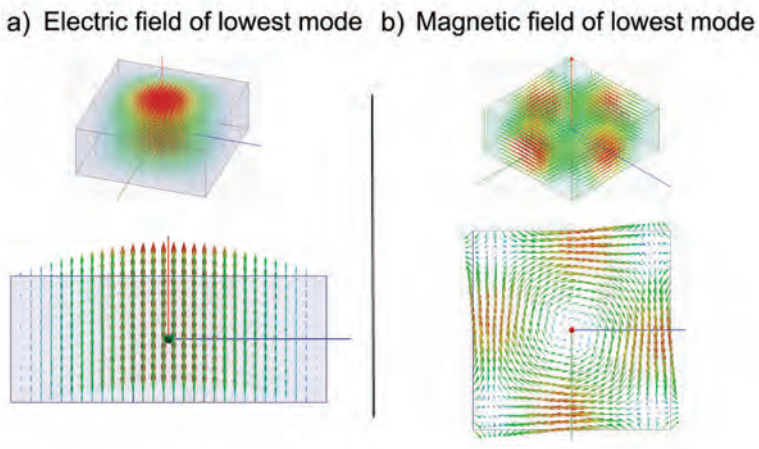

Figure 4

The simulated representation of the electric and magnetic field inside a box whose walls are conductors and inside is vacuum shows the maxima and minima of the fields in the cavity. a) The three dimensional view of the electric field demonstrates that the boundary condition $\mathbf{E}^{\parallel} = \mathbf{0}$ is satisfied. From the side view of the electric field, one can see that for the lowest mode, the electric field is maximum through the center of the cavity along the red-axis and minimized farthest away from the axis. b) Looking down the red-axis at the magnetic field, one can see that the boundary condition $B^{\perp} = 0$ is satisfied and the maximum of the magnetic fields occurs on the periphery of the cavity. Notice that the maxima for the electric and magnetic field occur in different locations.

C. Coupling between the Spin Ensemble and the Cavity

Section III A and Section III B describe the physics of two separate oscillators: a spin ensemble in a ruby crystal and a conducting cavity. Since spin is a magnetic phenomenon, the magnetic field in the cavity affects the spin ensemble. To achieve the strongest effect, the most coupling, one should maximize the amount of magnetic field in the ruby volume. (I would like to find a derivation of the coupling).[8]

D. Solenoid

As described in Section III A, the experiment needs a constant external magnetic field to tune to frequency of the spin waves. In order to do this, we use a solenoid made of Niobium wire, a superconductor. Previous research[6] suggests that the ruby will be degenerate with the cavity when the external magnetic field reaches about 30mT. The magnetic field produced by a solenoid at its center follows the equation

$$B = \frac{\mu NI}{L} \tag{10}$$

where N is the number of turns of wire, I is the current, μ is the magnetic permeability, and L is the length of the solenoid. The length of the solenoid must be large enough to create a constant magnetic field through the ruby, a requirement of the spin ensemble phenomenon. Calculating the magnetic field of a finite solenoid, I approximated 6 cm to provide a sufficiently constant magnetic field. Given that the maximum current that the wire can handle is 1 A (I would stay below this value), $N \geq 3000$ turns to achieve a good sweep through 30 mT. In fabrication, I found all of these parameters to be reasonable.

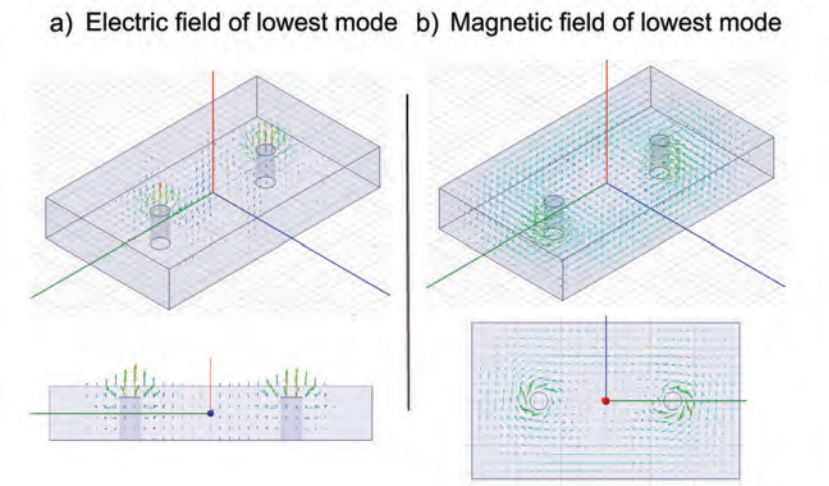

Figure 5

The modes for this cavity take a different shape due to the cylindrical, conductive extrusions in the interior. a) From the side, one can see that the electric field is maximized where the conductive walls become most close, at the top of the cylinders. The vectors pointing from the top of the cylinder to the roof mimic the pattern of the electric field for a parallel plate capacitor. b) The magnetic field maximum occurs closer to the bottom of the cavity. The concentric circles around the posts mimic the magnetic field vectors around a current carrying wire.

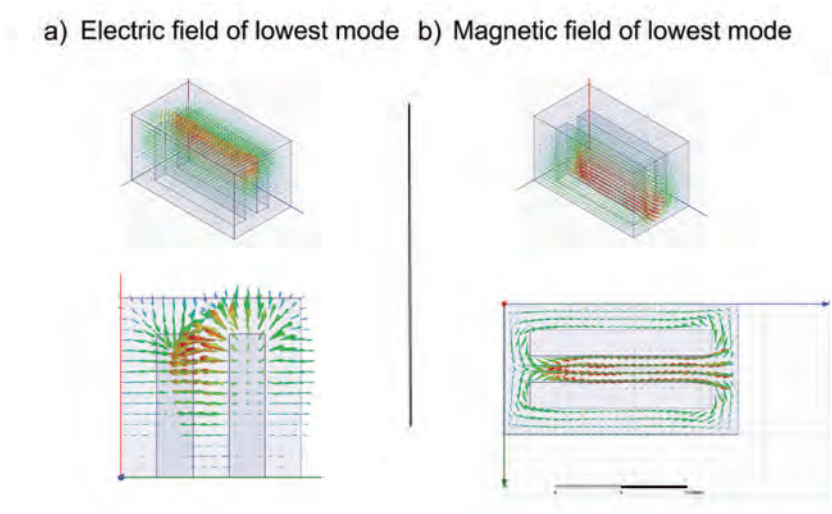

Figure 6

Similar to the cavity in *Figure 5*, the conducting rectangular posts shape the electric and magnetic fields. a) The electric field occurs near the top of the cavity with the vectors mimicking a parallel plate capacitor between the posts and the roof. b) The magnetic field maximum occurs near the bottom between the posts. The longer rectangle extrusions cause the magnetic field maximum to be evenly distributed in the middle of the two posts.

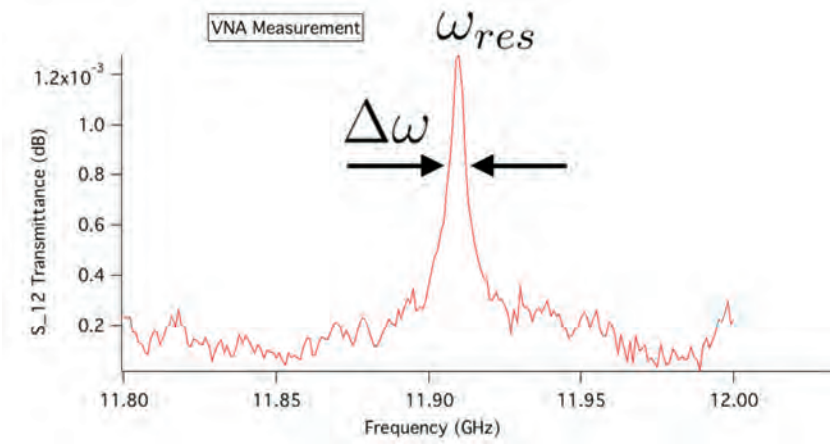

Figure 7

Output of Vector Network Analyzer (VNA) measurement of S_{12} for the double post cavity at roughly 0 K. Labels indicate the values that determine quality factor Q.

E. Data and Analysis

Understanding the underlying physics, one can now perform a simple experiment. Just like the experiment outlined in Section II, one can tune resonance of the spin ensemble with an external magnetic field created by a solenoid and observe the effect in the resonance of the cavity, which is electromagnetically coupled to the spin ensemble. To measure the resonance of the cavity, a Vector Network Analyzer (VNA) probes the cavity with a radio frequency signal through one antenna and observes the transmitted power in another. The power of transmittance between probe antennae in the cavity peaks at the resonance of the cavity (just like when you sing in the shower: a certain note resonates in the bathroom and sounds the loudest).

The graph of frequency versus transmitted power shown in *Figure 7* ideally follows a Lorentzian function. The maximum value and the full width at half of the maximum value parametrize the curve. These two values combine to give an important metric of a resonant cavity, the quality factor Q:

$$Q = \frac{\omega_{res}}{\Delta\omega} \tag{11}$$

where ω_{res} is the resonant frequency and $\Delta\omega$ is the full width half max as shown in *Figure 7*. A higher Q indicates a sharper resonant peak, which provides clearer data. Another definition of Q reveals another advantage of a higher quality factor:

$$Q = 2\pi \frac{\text{Energy Stored}}{\text{Energy Dissipated per Cycle}} \tag{12}$$

A resonator with higher Q has less energy loss. In fabrication, discussed later in Section IV, one should maximize the Q of both the cavity and spin ensemble.

Once we can tune the frequency of the spin ensemble and measure the resonance of the cavity, we can measure the effect of one on the other. I used the LabView programming language to orchestrate the experiment.

The experiment produces a 2D intensity plot of the transmitted power at a given external magnetic field and frequency (*Figure 8*). A vertical slice of the graph is an averaged VNA measurement like that in *Figure 7* at a given magnetic field. One should note that the experiment should be done slowly (about 1 second for a change in one mA) because rapid change though the current in the solenoid will heat up the fridge. This measurement that took a half hour heated the fridge from 9mK to 115mK.

To understand *Figure 8* better, consider how the resonant frequency changes with magnetic field. For low magnetic field the resonance (lightest spot) and Q (approximated by the width of the light patch) do not change, which is expected because the two oscillators' resonances begin far apart. As the magnetic field increases, which increases the ruby resonance, the Q decreases and the resonance changes. The Q gets so small at around 18 mT that the resonance of the cavity becomes difficult to measure. In this area, the two oscillators become intertwined such that one cannot measure them as separate oscillators; however, the VNA measures the cavity as if it were a separate oscillator. This discrepancy explains the change in Q. At around 25 mT the ruby resonance surpasses the cavity resonance enough so that the Q and resonance begin to return to normal. At larger magnetic field, which is unattainable with this experimental set up, the cavity resonance

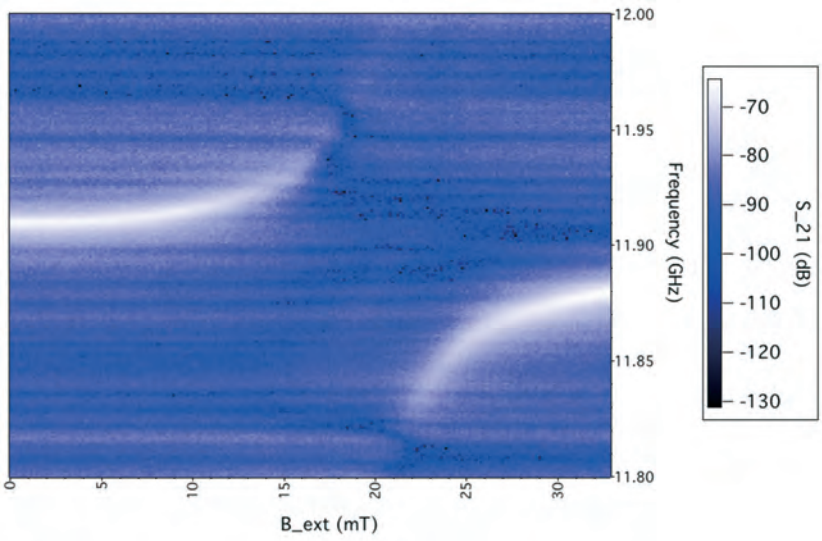

Figure 8
2D intensity plot of averaged VNA measurements at different magnetic fields.

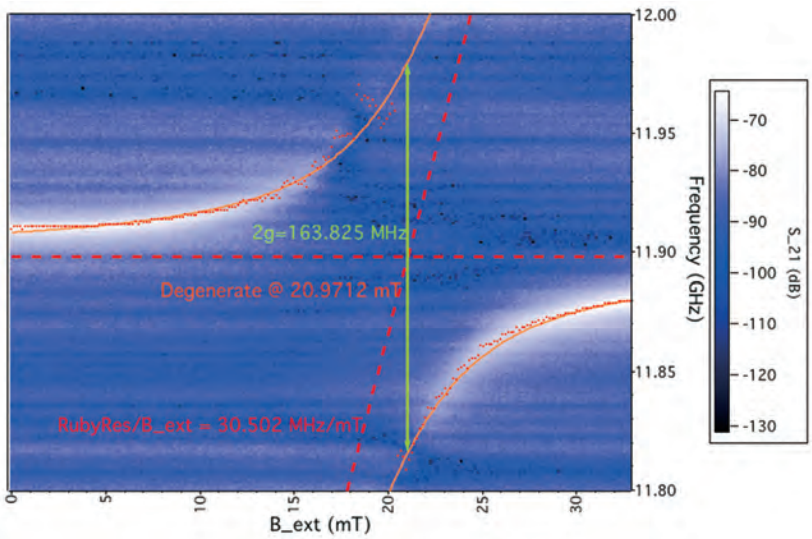

Figure 9
The data fits the avoided crossing curve, enabling a calculation of coupling strength *g*.

and Q would tend towards the values for an isolated cavity since the two oscillators grow very detuned in this limit.

The analysis of this data attempts to find the coupling strength, *g*, (see Section II) between the spin ensemble and cavity. Two curve fits provide independent approximations for *g*. One method uses the avoided crossing equation derived in Section II. The other method fits the data to an equation relating the Q of the cavity to external magnetic field, an equation used in similar crystal coupling experiments[6]. The results described below find similar values for *g* for the independent methods. Igor Pro facilitated the data analysis, graphing and curve fitting.

The first method fits the maxima of the VNA measurement at each magnetic field settingto the hyperbolic avoided crossing equation

$$f(x) = b(x-f) \pm \sqrt{(b(x-f))^2 + c} + d \tag{13}$$

where *b*, *f*, *c*, and *d* were fitting parameters. In reference to the avoided crossing graph in *Figure 9*, $2b$=30.502 MHz/mT is the slope of one asymptote, f=20.951 mT is the magnetic field strength at which the isolated resonances cross, $-d$= 11.898 is the resonance of the isolated cavity, and $\sqrt{c}/2 = g$ = 81:9125 MHz. Igor Pro allows one to simultaneously fit multiple sets of data to different equations using the same fitting parameters. Using this feature, the entire data set was fit to the avoided crossing curve, giving values for the these parameters as shown in *Figure 9*.

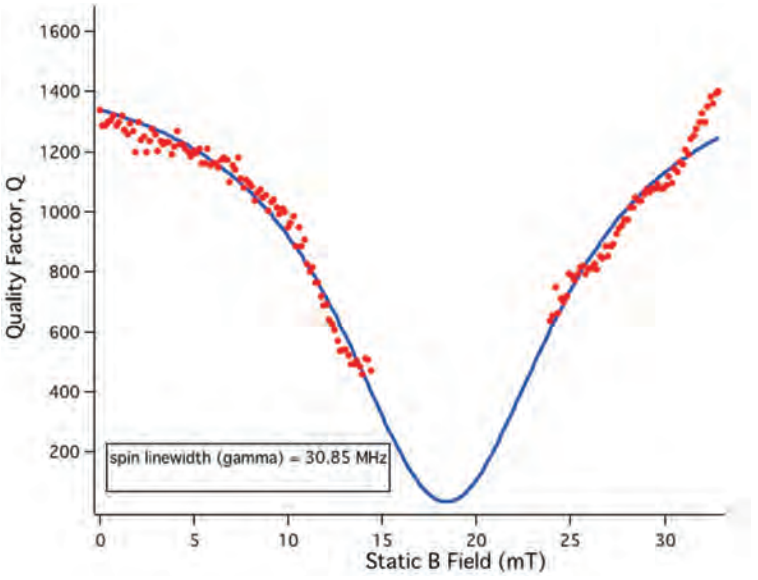

Figure 10: Quality Factor Dependence on Magnetic Field

The data in the small detuning range is discarded because Equation 15 only applies for large detuning. In other words, the peak in the VNA measurement becomes so indistinct that one cannot perform an accurate Lorentzian fit and therefore no Q.

The second method of finding g utilizes an equation that predicts the cavity Q as the resonance of the spin ensemble is changed:

$$Q = \frac{\Delta^2 + \gamma_2^{*2}}{2g_{s,eff}^2 \gamma_2^* + \kappa(\Delta^2 + \gamma_2^{*2})}\omega_r \tag{14}$$

In Equation 14, Δ, the detuning between the cavity and ruby resonances, is the independent variable. The cavity frequency $\omega_r/2\pi$ =11.89 GHz and the cavity linewidth $\kappa/2\pi$ =7.79 MHz are found far away from degeneracy and are constants in the curve fit. The collective coupling strength $g_{s,eff}/2\pi$ =74.84 MHz and the spin linewidth γ_2^* = 30.85 MHz, are extracted from the curve fit in *Figure 10*.

As you can see, the two values calculated for *g* are similar for this experiment. Comparing to a similar study[6], Schuster et al. found their cavity had $g_{s,eff}/2\pi$ =38 MHz, which implies less coupling in their 2D cavity. Also, their ruby had a spin linewidth γ_2^* = 96 MHz, which is wider than the result here.

The decrease in spin linewidth is promising, since that is the limitation on further applications of storing quantum information in spin ensembles.

IV BUILDING THE EXPERIMENT

A. Ruby Specifications

The ruby crystal was fabricated by Laser Materials Corporation. The shape is about 15mmx26mmx1mm with the axis of the ruby pointed along the longest length. The crystal is doped with 0.03 percent Cr_2O_3 by weight.

B. Milling a Cavity

This experiment requires a high Q cavity to attain strong coupling with the ruby spins. The Q of the cavity can be affected by the conductivity of the metal walls, smoothness of the metal walls, the shape of the cavity, the length of the probes, and impurities on the cavity walls. This cavity has a resonance of 11.9 GHz, a room temp Q of around 800 and a low temp Q of 1527. Copper was used for a few reasons. Mainly, copper does not superconduct and has a magnetic susceptibility close to vacuum, which allows an external magnetic field to easily pass through to interact with the spins to control Zeeman splitting. Superconductors have higher Qs since they have infinite conductivity, but the superconductors would either block the external magnetic field or fail to superconduct because of the external field. Copper also has a strong thermal conductivity, which cools the cavity and inner ruby to the base temperature of the dilution refrigerator. Copper is also easily machinable.

This cavity was sent to a company to machine it, but another option for making cavities that could be investigated is 3D printing metal cavities.

V CONCLUSION

Investigating a novel way to couple a ruby spin ensemble to a cavity, I found that the double post reentrant copper cavity improved coupling rate g and spin linewidth from

previous studies. These findings open new avenues to experiments with spin ensembles in crystals using similar cavity geometries.

References

[1] Zachary Burell. An Introduction to Quantum Computing using Cavity QED concepts. *arXiv preprint arXiv:1210.6512*, 2012.

[2] L. DiCarlo, J. M. Chow, J. M. Gambetta, Lev S. Bishop, B. R. Johnson, D. I. Schuster, J. Majer, A. Blais, L. Frunzio, S. M. Girvin, and R. J. Schoelkopf. Demonstration of two-qubit algorithms with a superconducting quantum processor. *Nature*, 460(7252):240–244, July 2009.

[3] David Griffiths. *Introduction to Electrodynamics*. Addison-Wesley, 4th edition, 2012.

[4] Atac Imamoglu. Cavity QED Based on Collective Magnetic Dipole Coupling: Spin Ensembles as Hybrid Two-Level Systems. *Physical Review Letters*, 102(8):083602, February 2009.

[5] Thornton Marion. *Classical Dynamics Of Particles And Systems Marion, Thornton.*

[6] D. I. Schuster, A. P. Sears, E. Ginossar, L. DiCarlo, L. Frunzio, J. J. L. Morton, H. Wu, G. A. D. Briggs, B. B. Buckley, D. D. Awschalom, and R. J. Schoelkopf. High-Cooperativity Coupling of Electron-Spin Ensembles to Superconducting Cavities. *Physical Review Letters*, 105(14):140501, September 2010.

[7] Daniel D. Stancil and Anil Prabhakar. Quantum Theory of Spin Waves. In *Spin Waves*, pages 33–66. Springer US, 2009. DOI: 10.1007/978-0-387-77865-5_2.